

Trends, stability and stress in the Colombian Central Andes

Daniel Ruiz · Douglas G. Martinson · Walter Vergara

Received: 28 July 2010 / Accepted: 15 August 2011 / Published online: 26 August 2011
© Springer Science+Business Media B.V. 2011

Abstract Mountain ecosystems have been projected to experience faster rates of warming than surrounding lowlands. These changes in climatic conditions could have significant impacts on high-altitude Andean environments, affecting the quality and magnitude of their economic and environmental services. Even though long-term data in these regions are limited, it is important to identify any discernible long-term trends in local climatic

Electronic supplementary material The online version of this article (doi:10.1007/s10584-011-0228-0) contains supplementary material, which is available to authorized users.

D. Ruiz

Programa en Ingeniería Ambiental, Escuela de Ingeniería de Antioquia, km 02 + 000 Vía al Aeropuerto José María Córdova, Municipio de Envigado, Antioquia, Colombia

D. Ruiz · D. G. Martinson

Department of Earth and Environmental Sciences, Columbia University in the City of New York, 1200 Amsterdam Avenue, 556-7 Schermerhorn Extension, New York, NY 10027, USA

D. G. Martinson

e-mail: dgm@ldeo.columbia.edu

URL: <http://www.ldeo.columbia.edu/>

D. Ruiz (✉)

International Research Institute for Climate and Society, Lamont-Doherty Earth Observatory, 61 Route 9W, PO Box 1000, Palisades, NY 10964-8000, USA
e-mail: pfcarlos@eia.edu.co

D. Ruiz

e-mail: pfcarlos@iri.columbia.edu

URL: www.eia.edu.co

D. G. Martinson

Lamont-Doherty Earth Observatory, Columbia University in the City of New York, 61 Route 9W, PO Box 1000, Palisades, NY 10964-8000, USA

W. Vergara

The World Bank, 1818 H Street, NW, Washington, DC, DC 20433, USA

e-mail: wvergara@worldbank.org

URL: <http://www.worldbank.org/>

conditions. Time series of several variables were analyzed to detect statistically significant long-term linear trends that occurred over recent years in a *páramo* ecosystem of the Colombian Central Andes. Records included cloud characteristics, sunshine, rainfall, minimum and maximum temperatures, diurnal temperature range, and relative humidity. Conditions of atmospheric stability were also explored. Total sunshine exhibited decreasing trends ranging from -3.7 to -8.5% per decade at altitudes around the pluviometric optimum. The strongest changes in sunshine occurred during the December–January–February season. Mean relative humidity observed at altitudes around and below this threshold showed increasing trends of $+0.6$ to $+0.7\%$ per decade. Annual rainfall and mean relative humidity above the optimum showed decreasing trends ranging from -7 to -11% per decade and from -1.5 to -3.6% per decade, respectively. Minimum temperatures on the coldest days and maximum temperatures on the warmest days exhibited increasing trends at all altitudes ranging from $+0.1$ to $+0.6$, and from $+0.2$ to $+1.1^\circ\text{C}$ per decade, respectively. Increases in minimum and maximum temperatures at higher altitudes were significantly greater than those observed in average at lower altitudes. The strongest changes in minimum temperatures, particularly, occurred during the December–January–February and June–July–August dry seasons. All these changes suggest that atmospheric conditions in the area are shifting from statically unstable conditions to conditionally unstable or statically stable conditions. Observed historical trends indicate that climate impacts and other human activities have stressed these unique and fragile environments.

1 Introduction

The upper range of the northern Andes harbors unique neo-tropical alpine wetland ecosystems locally known as *páramos*. They constitute exceptional grassland regions inhabiting the narrow altitudinal belt above the Andean cloud forests (the so-called bosque montano; ca. 2,000–3,500 m) and below the areas of “permanent” snow ($>$ ca. 4,500 m). *Páramos* provide numerous and valuable environmental goods and services including high biodiversity and a sustained (“regulated”) water supply for domestic, agricultural and industrial use (Buytaert et al. 2006), as well as for hydro-power generation in the region. For example, in Colombia, 80% of the water demand of its capital city, Bogotá, is supplied by a nearby *páramo*, and 67% of the installed power capacity is hydro-based. The historical climatic conditions of these ecosystems are characterized by average temperatures below 10°C , large diurnal temperature range, cloudy skies, foggy days, high UV radiation amounts, low atmospheric pressure, strong winds, and only drizzles (Castaño 2002; Gutiérrez et al. 2006; Ruiz et al. 2008). Some of these conditions have changed dramatically over recent decades.

Even though biophysical factors show considerable natural variability in the Andes, human activities occurring at local, regional and global scales have begun to introduce anthropogenic stress on high-altitude environments (Foster 2001; Diaz et al. 2003). Rapid environmental changes and important disruptions of the integrity of *páramo* ecosystems have been observed over recent years in Colombia (Castaño 2002; WBG 2006; Gutiérrez et al. 2006; Ruiz et al. 2008). Likely anthropogenically-induced changes include water stress during dry seasons due to receding glaciers and the disappearance of high-altitude water bodies, changes in patterns and abrupt loss of biodiversity, frequent occurrence and rapid spread of natural and human-induced fires, and increased erosion.

Although our understanding of glacier retreat and its consequences has significantly increased, the assessment of the consequences of climate change on the functioning of *páramos* and Andean forests requires additional work. In particular, improved knowledge

of rapid spatial and temporal changes in their climatic patterns and hydrological regimes has become a critical priority (WBG 2008). In this article we aim to investigate the recent changing climatic conditions experienced by the high mountain ecosystems inhabiting the El Ruiz–Tolima Volcanic Massif, on the Colombian Central Andes. We analyze historical time series of local climatic variables to detect statistically significant trends that occurred over recent years. This should lead to better documenting the conditions prevailing in these areas and to estimate the stress that these ecosystems are facing due to climate-induced changes. Our findings contribute to the ongoing design and implementation of the Colombian adaptation strategy, an effort that aims to preserve these unique, fragile, and strategic high-altitude environments that today provide valuable services, essential to the economy of the nation.

2 Study site

Analyses focus on the climatic conditions prevailing in the surroundings of the Claro River high-altitude basin, a mountain watershed located in the Los Nevados Natural Park, on the El Ruiz–Tolima Volcanic Massif, on the Colombian Andean Central Mountain Range-ACMR (see Fig. 1). Los Nevados is a protected area located within the spatial domain $04^{\circ}25'N$ – $05^{\circ}15'N$ and $75^{\circ}00'W$ – $76^{\circ}00'W$, in the Alto Cauca hydroclimatic region (DG-UNAL 2005), and more specifically, in the $04^{\circ}36'N$ – $04^{\circ}59'N$ and $75^{\circ}12'W$ – $75^{\circ}33'W$ domain. The

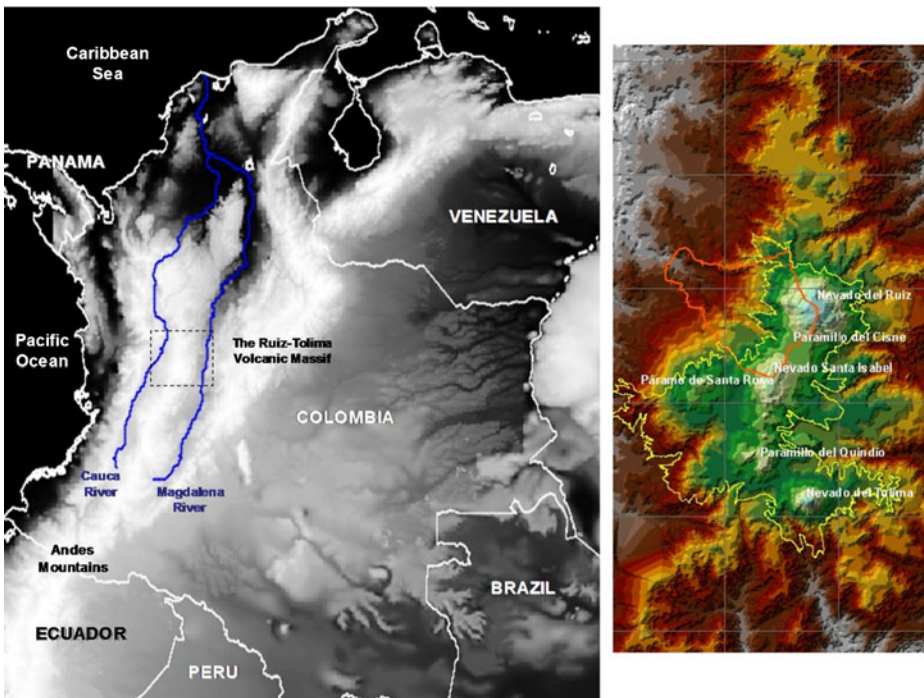


Fig. 1 Study site. Left panel: general location of the El Ruiz–Tolima Volcanic Massif, on the Colombian Andean Central Mountain Range (source of Digital Elevation Model: HidroSig Java; Copyright: Postgrado en Aprovechamiento de Recursos Hidráulicos, Universidad Nacional de Colombia Sede Medellín). Right panel: Claro River high-altitude basin (orange line) and Los Nevados Natural Park (yellow line) (source: Ruiz et al., 2008)

Claro River mountain basin, to approximately 1,800 m where the watercourse meets the Los Molinos River, lies in the region 04°48'N–04°58'N and 75°19'W–75°30'W and has a drainage area of about 191 km². The watershed is currently fed by numerous mountain streams originating high in the snowfields of the El Ruiz (5,321 m) and the Santa Isabel (5,100 m) ice-capped mountains.

3 Data

Analyzed records included satellite and ground meteorological data. Cloud characteristics (cloud amount, top pressure, top temperature, and optical thickness for multiple clouds), previously discussed by Ruiz et al. (2008), were processed for the grid point 03°45'N–76°15'W. These data can be downloaded from the Data Library of the International Research Institute for Climate and Society, IRI (<http://iri.columbia.edu/>; source: Rossow et al. 1996) and are discussed in Ruiz (2010). A total number of 37 weather stations, located in the spatial domain 04°25'N–05°15'N and 75°00'W–76°00'W, were also considered to assess local changing climatic conditions. Their datasets comprise daily, monthly and annual records of sunshine, rainfall, minimum and maximum temperatures, diurnal temperature range, and relative humidity. Data were provided by the Colombian Institute of Hydrology, Meteorology and Environmental Studies - IDEAM, the Central Hidroeléctrica de Caldas - CHEC, and the Centro Nacional de Investigaciones de Café-CENICAFE. Table 1 summarizes all the climatic datasets; the available historical periods of weather station data are presented in the [supplementary material](#). A detailed description of these records can be found in Ruiz (2009).

4 Methods

Daily time series (not all the datasets are available at a daily timescale) were checked for inconsistencies. Potential outliers were detected through simple run sequence plots. Anomalous records were expunged from the data before estimating monthly values only when there was strong evidence that they were erroneous (i.e. they were not reflecting the very nature of the climatic variable). However, a very small fraction of the available dataset was removed, as presented in the [supplementary material](#). Monthly time series were calculated for each of the climatic variables. The sample mean, median, mode, standard deviation, sample variance, standard error, kurtosis, skewness coefficient, range, minimum and maximum values, sample size, and confidence interval (95%) of each of the monthly time series were calculated using the Data Analysis Tool of Microsoft Excel. Annual cycles of cloud amount, top pressure and top temperature, optical thickness, sunshine, rainfall, minimum and maximum temperatures, diurnal temperature range, and relative humidity were calculated using the longest time series. Annual time series were calculated for each of the climatic variables. Exploratory analyses, including time series plots and box-plots, were conducted to detect non-homogeneities in annual (free of seasonality) time series. Confirmatory analyses were then implemented to assess the significance of the observed long-term linear trends. Trend magnitudes (slope parameters) were calculated by the method of least squares. Upper and lower confidence limits were also assessed for the simple linear regression models. Four statistical tests, namely the Student's *t*-test, the Hotelling–Pabst test, the non-parametric Mann–Kendall test (Kendall 1975), and the aligned rank Sen's *t*-test (Sen 1968), were all used to assess (at a $\alpha=0.05$) the null

Table 1 Summary of available ground meteorological data. The available historical periods of weather station data are presented in the [supplementary material](#)

Climatic variable	Climatic sub-variable	Longest historical period	
Sunshine	SR1	Total sunshine [hrs]	1955–2005
	SR2	Total number of foggy days/null sunshine [days]	
	TSD	Total number of sunny days [days]	
	SR4	Daily maximum sunshine [hrs]	
	SR5	Daily mean sunshine [hrs]	
	SR6	Daily minimum sunshine [hrs]	
	SR7	Day-to-day standard deviation of daily sunshine [hrs]	
Rainfall	R1	Total rainfall [mm]	1942–2006
	R2	Total number of dry days [days]	
	R3	Maximum daily rainfall [mm]	
Minimum temperature	MTmin	Minimum temperatures during the warmest days [°C]	1950–2007
	ATmin	Average minimum temperatures [°C]	
	mTmin2	Minimum temperatures during the coldest days [°C]	
	SDTmin	Day-to-day standard deviation of minimum temperatures [°C]	
Maximum temperature	MTmax	Maximum temperatures during the warmest days [°C]	1950–2007
	ATmax	Average maximum temperatures [°C]	
	mTmax2	Maximum temperatures during the coldest days [°C]	
	SDTmax	Day-to-day standard deviation of maximum temperatures [°C]	
Diurnal temperature range	MDTR	Maximum diurnal temperature range [°C]	1950–2007
	ADTR	Mean diurnal temperature range [°C]	
	mDTR2	Minimum diurnal temperature range [°C]	
	SDDTR	Day-to-day standard deviation of diurnal temperature range [°C]	
Relative humidity	MRH	Maximum relative humidity [%]	1950–2007
	ARH	Mean relative humidity [%]	
	mRH2	Minimum relative humidity [%]	
	SDRH	Day-to-day standard deviation of relative humidity [%]	

hypothesis of zero slope parameters in the annual time series. A historical time series was considered to have a statistically significant long-term linear trend in the mean at a $\alpha=0.05$ significance level when at least three of the hypothesis tests rejected the null hypothesis of a zero slope parameter. Serially independent yearly time series were assumed when implementing the non-parametric Mann–Kendall test. December–January–February, March–April–May, June–July–August, and September–October–November time series (see [supplementary material](#) for the case of total sunshine and minimum

temperatures on the coldest days), as well as monthly records of sunshine, rainfall, minimum, mean and maximum temperature, diurnal temperature range, and relative humidity gathered at the weather station XII (ID 2615502), were also processed to support the analysis (see [supplementary material](#)). Weather station XII was chosen because its observational periods span the longest historical periods of the available dataset. All hypothesis tests were run using the Analysis of Historical Time Series (ASH) software developed by J.D. Salas and R.A. Smith at the Hydrology and Water Resources Program, Colorado State University, and recently modified at the Water Resources Graduate Program, National University of Colombia at Medellin. Finally, long-term trends, statistically significant at a $\alpha=0.05$, were plotted on a map of the $04^{\circ}25'N-05^{\circ}15'N$ and $75^{\circ}00'W-76^{\circ}00'W$ spatial domain, and in the vertical profiles of sunshine, rainfall, temperature, and water content.

Topographic profiles of the Claro River were created using a high-resolution digital terrain model produced from 1:25.000 scaled digital elevation contour maps (Ruiz et al. 2008). Average values of mean and minimum annual temperatures, annual dew point, actual and saturation vapor pressures, atmospheric pressure, actual and saturation mixing ratios, relative humidity, and potential temperature were computed for different altitudes (see spatial distributions in Ruiz et al. 2008). Saturation and actual mixing ratios were estimated through the Clausius–Clapeyron equation for the inferred spatial distributions of mean annual temperature and mean annual dew point, respectively. The Lifting Condensation Levels (LCLs) were estimated by comparing the vertical profiles of mixing and saturation mixing ratios. Finally, the vertical profile of mean annual temperature (environmental lapse rate) was compared to the theoretical paths of dry and moist adiabatic lapse rates and to the trends in minimum and maximum local temperatures, to characterize local climatic conditions and to define the regions of static instability, static stability, and conditional instability. A statically unstable atmosphere is characterized by vertical motions, the formation of convective currents, turbulence and mixing of air layers. In a statically stable atmosphere, vertical motions are inhibited, air layers are stratified and consequently free from convection, and air masses exhibit a low degree of turbulence. In a conditional unstable atmosphere, the air is unsaturated and could become unstable on the condition it becomes saturated.

5 Results

The discussion presented here includes only those long-term linear trends that are statistically significant at a 0.05 significance level.

5.1 Cloud characteristics and sunshine

The mean annual values of all-type cloud amount, top pressure, top temperature, and optical thickness, observed over the grid point $03^{\circ}45'N-76^{\circ}15'W$ during the period 1983–2001, reached 80.6%, 438 mb, 256 K, and 7.56, respectively. The annual values of sunshine variables are presented in Table 2.

A decrease in all-type cloud cover of about 1.9% per decade (homogeneous, not geometric) was detected over the observing period. Trends in the mean of the historical time series of mean annual cloud top pressure, top temperature and optical depth were not observed over the available historical period. As for sunshine, the top left panel of Fig. 2 depicts the annual values and long-term trends of the total annual

Table 2 Annual historical values of sunshine variables

Area	SR1 [hours/year]	SR2 [days/year]	TSD [days/year]	SR4 [hours/day]	SR5 [hours/day]	SR6 [hours/day]	SR7 [hours/day]
Lower altitudes on the W flank of the ACMR	1,330–1,750	8–11	344–357	8.9–9.5	4.1–4.9	0.27–0.38	2.4–2.6
Higher altitudes on the W flank of the ACMR	760	53	268	8.1	2.5	0.01	2.3
Lower altitudes on the E flank of the ACMR	1,550–1,600	12	341–351	9.4–9.6	4.3–4.6	0.22–0.27	2.6–2.7

sunshine (SR1) observed in the selected spatial domain. SR1 values gathered at most of the weather stations located on the western flank of the ACMR at altitudes around the so-called pluviometric optimum (ca. 1,500 m; Hastenrath 1991; Oster 1979) exhibited statistically significant decreasing trends ranging from -3.7 to -8.5% per decade, i.e. from -65 to -120 h per decade, approximately. Weather stations located above that

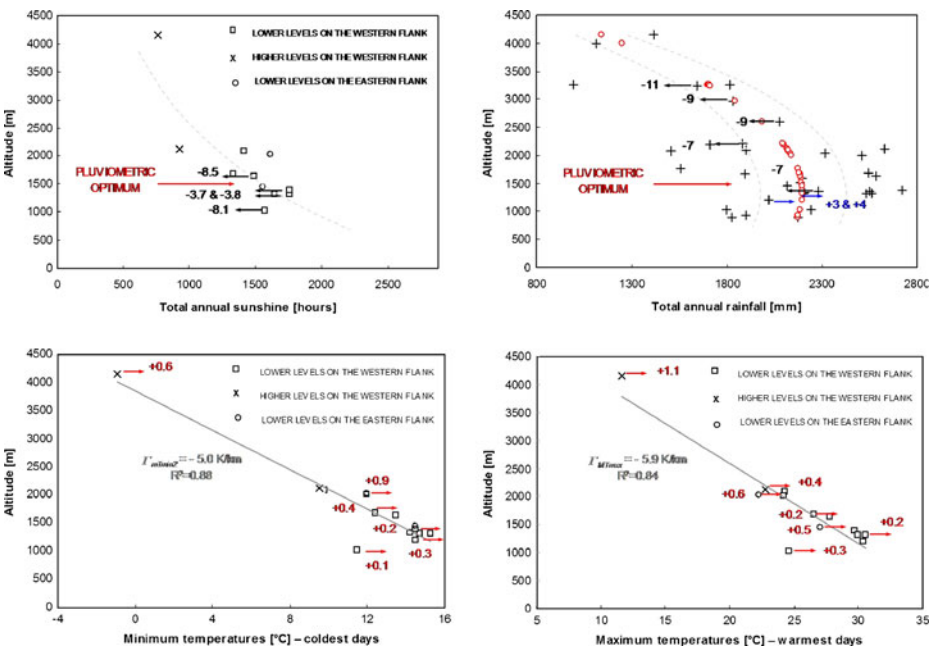


Fig. 2 Historical annual values (boxes, crosses and circles) of sunshine (top left panel), rainfall (top right panel), minimum temperatures on the coldest days (bottom left panel), and maximum temperatures on the warmest days (bottom right panel) observed in the spatial domain $04^{\circ}25'N-05^{\circ}15'N$ and $75^{\circ}00'W-76^{\circ}00'W$. Grey dashed and solid lines in top left, bottom left and bottom right panels depict the observed patterns in vertical profiles. I_{MTmin2} and I_{MTmax} in bottom left and right panels represent the adjusted lapse rates; see also the R-squared coefficient, which depicts the measure of the fit. Red circles in the top right panel depict the observed pattern of total annual rainfall with altitude. Grey dashed lines in the top right panel represent the observed envelopes. Arrows on top of all panels represent the observed long-term linear trends that were statistically significant at a 95% confidence level (boxes, crosses and circles without arrows depict those weather stations that reported climatic records with long-term trends that were not statistically significant at a 0.05 significance level). Trends in sunshine and rainfall (values next to arrows) are expressed in %/decade; trends in temperature (values next to arrows) are expressed in $^{\circ}C$ /decade. Black arrows pointing to the left in top left and right panels depict decreasing trends. Blue arrows pointing to the right in top right panel depict increasing trends. Red arrows pointing to the right in bottom left and right panels represent increasing trends

optimum did not experience increasing/decreasing trends. The strongest changes in the total sunshine occurred during the December–January–February season, as presented in the [supplementary material](#). Decreases in SR1 are consistent with statistically significant increases in the total number of foggy days (or decreases in the total number of sunny days) of about +1.0 to +2.3 days per decade that were observed at the same weather stations. Daily maximum, mean and minimum sunshine values observed at lower altitudes also exhibited decreases of about –0.1 to –0.4, –0.2 to –0.4, and –0.08 to –0.1 h/day/decade, respectively.

5.2 Rainfall

The annual values of rainfall variables are presented in Table 3. The top right panel of Fig. 2 depicts the annual values and long-term trends of the total annual rainfall (R1) observed in the selected spatial domain. R1 amounts showed statistically significant decreasing trends ranging from –7 to –11% per decade (homogeneous, not geometric), i.e. –135 to –180 mm per decade, in some met stations located at altitudes above the pluviometric optimum and particularly over the western flank of the ACMR. Below this level, the historical time series of only two weather stations exhibited increasing trends of about +3 to +4% per decade; i.e. +63 to +87 mm per decade. Most of the weather stations gathering the total number of dry days did not show statistically significant increasing/decreasing trends. Finally, maximum daily precipitation records suggested an increased occurrence of unusually heavy rainfall events, particularly over the western flank of the ACMR, with trends in the mean of about +1 to +4% per decade, equivalent to +0.7 to +2 mm per decade.

5.3 Minimum and maximum temperatures

The annual values of minimum and maximum temperature variables are shown in Table 4. Minimum temperatures on the warmest days (MTmin) exhibited statistically significant trends at lower altitudes that range from +0.1 to +0.2°C per decade. MTmin records gathered at higher altitudes did not show significant trends. Average minimum temperatures (ATmin) gathered at weather stations located at lower altitudes exhibited increasing trends that range from +0.1 to +0.3°C per decade. ATmin records observed at higher altitudes did not show significant trends. Minimum temperatures on the coldest days exhibited statistically significant increasing trends at all altitudes that range from +0.1 to +0.6°C per decade (see bottom left panel of Figs. 2 and 3). Increases in these extreme temperatures at higher altitudes were almost twice of what was observed in average at lower altitudes. Also, the strongest changes in the minimum temperatures on the coldest days occurred during the December–January–February and June–July–August dry seasons, as presented in the [supplementary material](#).

Table 3 Annual historical values of rainfall variables

Area	R1 [mm/year]	R2 [days/year]	R3 [mm/day]
Lower altitudes on the W flank of the ACMR	1,800–2,700	106–187	42.7–48.0
Higher altitudes on the W flank of the ACMR	1,100–2,000	120–173	19.5–31.7
Lower altitudes on the E flank of the ACMR	1,900–2,300	153	45.7
Higher altitudes on the E flank of the ACMR	990–1,800	193–199	18.1–32.3

Table 4 Annual historical values of temperature, diurnal temperature range and relative humidity variables. The Greek letter ‘ Γ ’ represents the adjusted lapse rates (changes in temperature with increases in altitude); see also the R-squared coefficient, which depicts the measure of the fit

Climatic variable	Sub-variable	Min	Max	Climatic variable	Sub-variable	Min	Max
Minimum temperatures [°C]	MTmin $\Gamma=-4.9$ K/km ($R^2=0.88$)	+3.0	+18.6	Maximum temperatures [°C]	MTmax $\Gamma=-5.9$ K/km ($R^2=0.84$)	+11.6	+30.6
	ATmin	+1.2	+17.2		ATmax	+8.4	+27.7
	mTmin2 $\Gamma=-5.0$ K/km ($R^2=0.88$)	-1.5	+15.3		mTmax2 $\Gamma=-5.5$ K/km ($R^2=0.86$)	+5.5	+23.5
	SDTmin	+0.8	+1.0		SDTmax	+1.2	+1.9
Diurnal temperature range [°C]	MDTR	9.3	14.7	Relative humidity [%]	MRH	90.2	98.2
	ADTR	6.6	11.0		ARH	74.5	91.6
	mDTR2	3.6	6.3		mRH2	62.7	77.1
	SDDTR	1.4	2.1		SDRH	4.8	7.2

Maximum temperatures on the warmest days exhibited statistically significant trends at all altitudes that ranged from +0.2 to +1.1°C per decade (see bottom right panel of Fig. 2). Increases at higher altitudes were more than three times what was observed in average at lower altitudes. Average maximum temperatures exhibited increasing trends that range from +0.2 in average at lower altitudes to +1.0°C per decade at higher altitudes. Maximum temperatures on the coldest days exhibited statistically significant increasing trends in only three weather stations; their increasing trends in the mean reached +0.2, +0.3, and +0.9°C per decade, respectively.

5.4 Diurnal temperature range

The annual values of diurnal temperature range (DTR) variables are shown in Table 4. Statistically significant increasing trends of about +0.4 to +1.2°C per decade were observed in maximum DTRs at higher altitudes, whereas at lower altitudes decreasing trends of about -0.2 to -0.4°C per decade were detected. Average DTRs showed increasing trends of +0.3 and +1.3°C per decade at altitudes above 2,000 m, and decreasing trends of about -0.2 and -0.3°C per decade at altitudes in the range [1,000–2,000 m]. Minimum DTRs exhibited statistically significant trends of about +1.0°C per decade at higher altitudes and decreasing trends of about -0.1 to -0.3°C per decade at altitudes below 2,000 m.

5.5 Relative humidity

The annual values of relative humidity (RH) variables are shown in Table 4. Statistically significant trends in maximum RH were only seen in the records of three weather stations, whose historical trends reached -2.2% per decade at higher altitudes, and +3.0 and +2.4% per decade at lower altitudes. Average RH records exhibited statistically significant decreasing trends at altitudes above the pluviometric optimum ranging from -1.5 to -3.6% per decade. Some weather stations located at altitudes around and below this threshold showed statistically significant increasing trends of about +0.6 to +0.7% per decade. Minimum RH records exhibited statistically significant decreasing trends that range from -3.2 to -8.7% per decade; only one weather station showed records with an increasing trend of about +1.2% per decade.

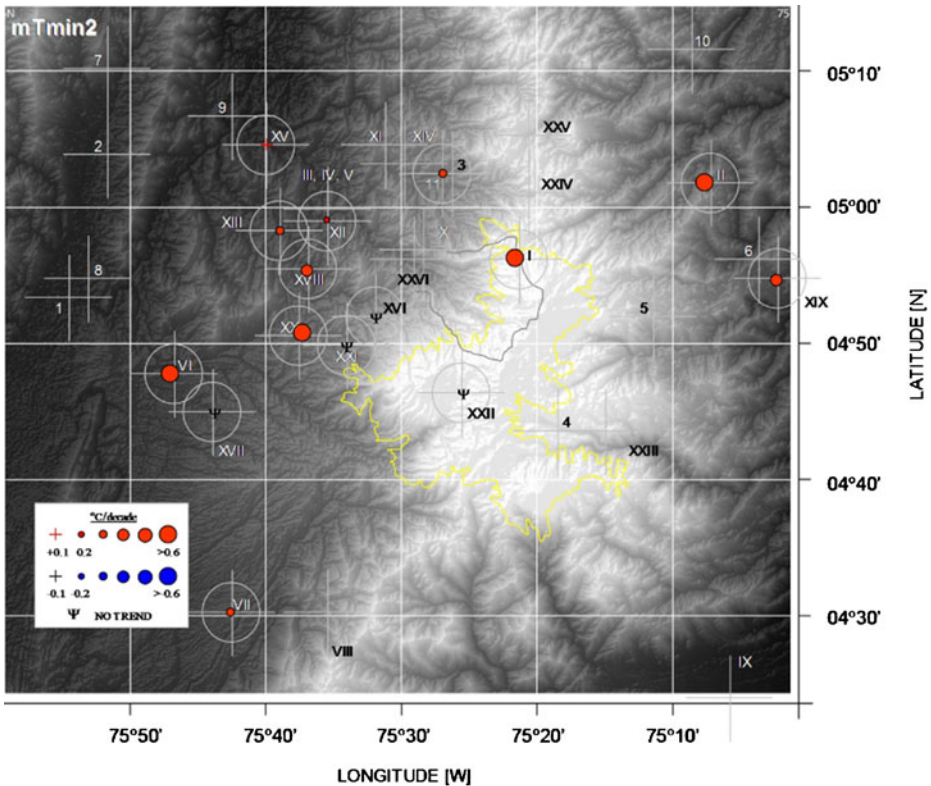


Fig. 3 Estimated long-term trends in the mean (confirmatory analysis) of minimum temperatures observed on the coldest days in the selected spatial domain (04°25'N–05°15'N and 75°00'W–76°00'W). Crosses represent the location of meteorological stations. Grey circles around crosses denote those weather stations with available records of minimum temperatures. Trends plotted with red and blue circles are significant at a 95% confidence level. The size of these circles depicts the rate of change (see labels). Greek letter Ψ depicts those weather stations that reported climatic records with long-term trends that were not statistically significant at a 0.05 significance level. Yellow solid line delineates the perimeter of the Los Nevados Natural Park; grey solid line shows the Claro River high-altitude basin

5.6 Atmospheric stability in the area of the Claro River watershed

Table 5 summarizes the estimated climatic conditions along the mainstream of the Claro River watershed. Figure 4 depicts the estimated regions of static instability, conditional instability, and static stability in the area of this high-altitude watershed. As mentioned before, increasing trends in extreme temperatures at higher altitudes (which would be depicted by right-ward shifts in the mean values of each box-plot in Fig. 4) are significantly greater than those observed at lower altitudes. Particularly, minimum temperatures on the coldest days in the headwaters have increased at a rate greater than +0.6°C per decade, whereas at lower altitudes the increasing trend only reaches +0.2 to +0.3°C per decade over the same period of time. Maximum temperatures on the warmest days have increased over the past two decades at an extraordinary rate of +1.5°C per decade in the headwaters, whereas at lower altitudes the trend only reaches +0.2 to +0.3°C per decade. Also, changes in the variance (which would be depicted by broadening/contraction of range in each box-plot) are significantly

Table 5 Climatic conditions along the mainstream of the Claro River watershed

Climatic variable	Lower altitudes, ~1,800 m (Claro River–Molino River confluence)	Higher altitudes, ~4,450 m (Visible headwaters)
Mean annual temperature [°C]	+19.9	+3.2
Minimum annual temperature [°C]	+13.1	–2.3
Mean annual dew point [°C]	+14.6	+0.9
Annual actual vapor pressure [hPa]	16.6	6.5
Annual saturation vapor pressure [hPa]	20.5	7.7
Mean annual relative humidity [%]	81.5	85.1
Atmospheric pressure [mb]	814.6	602.6
Actual mixing ratio	0.0127	0.0067
Saturation mixing ratio	0.0156	0.0079
Potential temperature [K]	274.1	239.1

greater at higher altitudes: the day-to-day standard deviation of maximum temperatures observed in the headwaters of the Claro River have increased at a rate of +0.3°C per decade, whereas in the lowlands the increasing trend reaches +0.1°C per decade.

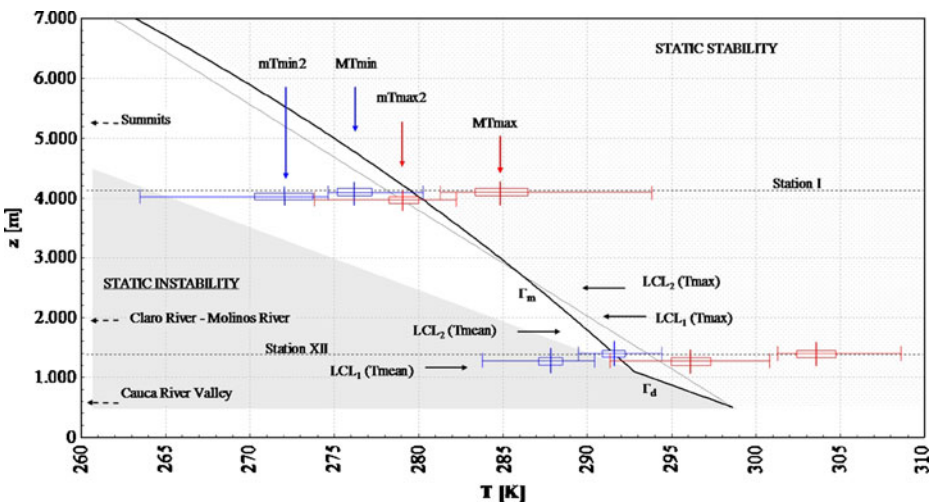


Fig. 4 Estimated regions of static instability, conditional instability, and static stability in the area of the Claro River watershed. Γ_d and Γ_m represent the dry and moist (saturated) adiabatic lapse rates, respectively. LCL_1 and LCL_2 denote the estimated Lifting Condensation Levels for air parcels located at altitudes of around 700 m (Cauca River Valley) and 1,310 m (foothills of the ACMR or around met station XII), respectively. Shaded and dotted areas represent, respectively, the regions of static instability (environmental lapse rate is greater than Γ_d) and static stability (environmental lapse rate is smaller than Γ_d and Γ_m). The white area between the abovementioned areas depicts the region of conditional (in)stability (environmental lapse rate is between Γ_d and Γ_m). In this graph, regions of static instability, conditional instability and static stability are delimited assuming a LCL at an altitude of $LCL_1(T_{mean})$. Observed temperatures are represented by box-plots: blue for minimum monthly temperatures; red for maximum monthly temperatures. In each box-plot, vertical lines depict, from left to right, the minimum, mean and maximum observed values; boxes represent +1.0 standard deviations. mT_{min2} and MT_{min} represent the minimum monthly temperatures during the coldest days and the warmest days, respectively; mT_{max2} and MT_{max} represent the maximum monthly temperatures during the coldest and the warmest days, respectively

6 Discussion and conclusions

Climatic patterns have changed in the central region of the ACMR. Observed trends in several climatic variables and inferred conditions of atmospheric (in)stability suggest that climatic stress is increasing in the high-altitude Andean ecosystems of the Central Cordillera. Some key aspects of the inferred and observed changes are discussed below.

6.1 Changes in atmospheric stability

Atmospheric stability conditions in the area of the Claro River watershed are characterized by the following factors: (a) cloud and fog formation in montane cloud forests, (b) moist advection over the western flank of the ACMR during day-time uplifting thermodynamic processes, and (c) cooling and drying processes driven by nighttime down-slope winds (nocturnal subsidence dynamics). Air masses' daytime motions play a significant role in the integrity of high-altitude ecosystems and are considered key to the preservation of high-altitude environments (Ruiz et al. 2008). The process seems to be simple: in the early morning when the lower atmosphere is statically stable, low- and middle-level clouds are clearly differentiated from their high-level counterparts. With solar insolation heating the ground surface during the first hours of the day, enough convective potential energy is accumulated in the lower altitudes of the atmosphere to destabilize this condition (Vernekar et al. 2003). In the late morning and early afternoon, statically unstable conditions prevail, producing turbulence and vertical mixing. The induced atmospheric motions transport significant amounts of water vapor from lower to higher altitudes in the lower atmosphere, increasing the relative humidity in high-altitude environments, forming fog and middle-level clouds, and initiating convective cloud clusters. Fog and middle-level clouds protect the vegetation, ice-caps, high-altitude water bodies, and aquatic microhabitats from direct sunlight. Differences in temperature and humidity between higher and lower altitudes control the diurnal dynamics, and would likely continue to drive future climate conditions in this high mountain environment.

Analyses indicate that ambient temperatures at higher altitudes are increasing significantly faster than those observed in lowland weather stations, a difference that is consistent with the outputs of several General Circulation Models (Trenberth et al. 2007; Meehl et al. 2007). Also, relative humidity records in higher altitudes exhibited strong reductions, compared to the weak but significant increasing trends observed at lower altitudes. Even though several other factors, such as changes in circulation dynamics and land conversion on the west flank of the Cordillera Central must be also considered for the analyses of alterations in atmospheric stability in the area, it can be argued that the observed increases in near-surface temperatures at higher altitudes are strongly affecting the relationship between the environmental lapse rate and the dry and moist adiabatic lapse rates. The current scenario suggests that this section of the atmosphere is increasingly becoming conditionally unstable or statically stable. Hence, currents of uplifting air, commonly occurring in the area during the late morning and early afternoon, could be progressively weakening. As a consequence of this disruptive process, less water vapor is being produced over Andean cloud forests and less fog could be reaching higher altitudes on these mountains (Ruiz et al. 2008).

Changes in the amount of cloud and fog cover, driven by changes in atmospheric stability, have significant impacts on the net radiation balance, and consequently on glacier masses, high altitude water bodies and mountain species. Our analyses suggest important reductions in the amount of all-type clouds over the observing period. As satellite data only

capture information from the highest cloud tops, only those changes that have occurred in the amount of low-level clouds that are not obscured by higher clouds can be addressed (A. Del Genio, personal communication). This limitation indicates that the observed decreasing trend is a lower limit of what has been happening in the area; thus, low-level clouds might have decreased even more. Our previous study (Ruiz et al. 2008) reported that in higher altitudes (ca. 4,150 m) the total number of foggy days per month has slightly decreased over the past two decades, and hence, the total number of sunny days per month has increased. Analyses presented here suggest that decreases in the total annual sunshine, the total number of sunny days, and the maximum, minimum, and mean daily sunshine values have occurred at lower altitudes. Also, we detect increases in the total number of days of null sunshine. Again, these evidences suggest that the mechanism that moves water vapor to higher altitudes has probably weakened over recent decades. In lower altitudes fog is more and more often getting “trapped”, increasing the occurrence of foggy days there. In higher altitudes, decreases in fog, evidenced by decreases in relative humidity, could be the mechanism behind the increases in the number of sunny days. This scenario is particularly harmful to páramo life zones because without fog they are “protected” from direct sunlight only by high-level clouds, which have the net effect of increasing surface temperatures. Although deep convective events are expected to become less frequent (A. Del Genio, personal communication), analyses of minimum monthly temperatures at higher altitudes suggest that they have not changed as dramatically as maximum monthly temperatures, thus the reason why the atmosphere still exhibits strong movements of uplifting air in several instances. Thus, deep convective events could occur when conditions at the ground become favorable moisture-wise.

6.2 Observed trends in rainfall and temperature

Although studies on changing climatic conditions in páramo life zones are limited due to the lack of long-term historical records, there is considerable evidence suggesting that significant changes in annual rainfall and near-surface ambient temperatures have occurred in these tropical environments. Bradley et al. (2006) analyzed temperature records gathered at several climatic stations along the Tropical Andes and indicated that the rate of increase in air temperatures reached $+0.11^{\circ}\text{C}$ per decade over the period from 1939 to 1998. If continued, this trend suggests that mean annual ambient temperatures in the headwaters of the Claro River could reach 5.4°C by 2050 (i.e. an increase of almost 0.6°C over the mean value of 4.9°C observed during the period 1981–2003). For Colombia, Pabón (2003 and 2004) analyzed weather stations data and indicated that total annual rainfall over the period 1961–1990 changed (increased or decreased) at rates of 4 to 6% per decade, and mean annual ambient temperatures increased at rates of about $+0.1$ to $+0.2^{\circ}\text{C}$ per decade over the same period. By assuming the maximum observed trend ($+0.2^{\circ}\text{C}$ per decade) mean annual temperatures in the headwaters of the Claro River could reach 5.9°C by 2050. More recent analyses (Departamento de Geografía–Universidad Nacional de Colombia 2005) have suggested that changes in precipitation in the Alto Cauca hydroclimatic region exceeded -2.4% , with respect to the 1961–1990 normal annual rainfall, and increases in near-surface temperatures reached $+0.12^{\circ}\text{C}$ per decade over the same period. Extrapolations of such detected trends suggest a decrease in total annual rainfall in the area of 14% and an increase in temperature of about $+0.7^{\circ}\text{C}$ by 2050, both with respect to the total and mean values observed over the period 1961–1990. Consequently, mean annual ambient temperatures in the headwaters could reach 5.5°C in 50 years. In summary, previous estimates suggest that near-surface air temperatures in the high mountain basin of the Claro River are likely to reach from 5.4 to 5.9°C by 2050. Our study has

produced evidence supporting these findings: temperature data observed in the surroundings of the Claro River watershed suggest that mean annual temperatures have increased coherently at rates ranging between +0.2 and +0.4°C per decade, while minimum and maximum annual temperatures have increased at rates of about +0.4 to +0.6°C per decade. Under these conditions, we suggest that mean annual ambient temperatures in the headwaters of the Claro River could reach an extremely high value for these environments of 7.0°C by 2050.

6.3 Other changes

Previous studies have reported that, due to increases in tropospheric aerosol concentrations in the atmosphere, the diurnal temperature range (DTR) is decreasing in several places around the world. Our analyses suggest that maximum, mean, and minimum DTRs at higher altitudes have increased over the past decades. This upward trend is a consequence of the difference between the rates of increase in minimum and maximum temperatures. Also, cold days are becoming less frequent in the area. Analyses of available records suggest that minimum and maximum temperatures during the coldest days have significantly increased over recent decades. Furthermore, we observed changes in the variability of extreme temperatures. Historical time series of minimum temperatures exhibited a decrease in the variance, whereas maximum temperatures showed an increase. All these changes could favor the colonization of several mountain species, but might have a devastating impact on those individuals that have adapted to extreme conditions and now require them.

In summary, changing climatic conditions are now seriously contributing to increased stress on the high mountain ecosystems of the Colombian Central Mountain Range. The observed changes 'are currently occurring region-wide, are cumulative, and are likely to be irreversible' (WBG 2008). Also, model projections (not discussed here) consistently suggest future climatic conditions would be unfavorable for páramo life zones (Vuille et al. 2003; Diaz et al. 2003). Although their impacts on the integrity of high-altitude habitats are very difficult to assess, our analyses suggest that changing climatic conditions could lead to the disruption of páramo ecosystems. Some of the expected impacts include: (a) upward migrations of low-altitude plant species and upward shifts of ecosystem boundaries (Gutiérrez 2002), reducing the extent of páramo habitats; (b) increase in the rate of desertification of mountain habitats, due to the altitudinal changes in sunshine and rainfall; (c) additional retreat of glacier margins and reduction in mountains' water regulation capacity, due to increases in precipitation in the form of heavy rain. All these impacts, combined, constitute a serious threat to unique high-altitude habitats and, consequently, to the water supply in the region. A reduction in water availability for human consumption in urban centers, agricultural and industrial use, and hydro-power generation could affect vital elements of the economy and welfare of the nation. In the foreseeable future it will be more expensive to supply water for these demands (WBG 2008). Undoubtedly, ambitious sustainable management strategies are now urgently required to protect these unique, rich, fragile, and highly endangered environments.

Acknowledgements The authors wish to thank A. Del Genio, D. Rind and A. Lacis (NASA Goddard Institute for Space Studies at Columbia University in the City of New York), M. Cane (Lamont-Doherty Earth Observatory, Columbia University in the City of New York), A. Jaramillo (Centro Nacional de Investigaciones de Café - CENICAFE) and C. Tobón (Departamento de Ciencias Forestales, Universidad Nacional de Colombia Sede Medellín) for their valuable comments. The research group thank the Colombian Institute of Hydrology, Meteorology and Environmental Studies - IDEAM, the Central Hidroeléctrica de Caldas - CHEC, the Centro Nacional de Investigaciones de Café - CENICAFE, the Corporación Autónoma Regional de Caldas - CORPOCALDAS, the Corporación Autónoma Regional de Risaralda - CARDER, the Instituto Geográfico Agustín Codazzi - IGAC, and the Unidad Administrativa Especial del Sistema de

Parques Nacionales Naturales de Colombia - UAESPNN for providing data and continuous support. The group also acknowledges the following individuals for their assistance during field campaigns: the rangers of the Los Nevados Natural Park (special thanks go to M. H. Arias and J. B. de la Cruz), the guides of the Asociación Caldense de Guías (special thanks go to A. Mayorga), L. F. Giraldo (Eco-Turismo Estratégico) and A. Tibaguy, and all the employees of the Tourist Services of the Los Nevados Natural Park (Concesión Nevados). We also acknowledge the helpful suggestions made by three anonymous peer-reviewers who read and commented this manuscript. Research activities were supported by the World Bank Group (Contract 7147577: Signals of climate variability/change in surface water supply of high-mountain watersheds. Case study: Claro River high mountain basin, Los Nevados Natural Park, Andean Central Mountain Range) and the Programa en Ingeniería Ambiental, Escuela de Ingeniería de Antioquia (Colombia). DRuiz was partially supported by the Department of Earth and Environmental Sciences (Columbia University in the City of New York) and the International Research Institute for Climate and Society, Lamont–Doherty Earth Observatory.

References

- Bradley RS, Vuille M, Diaz HF, Vergara W (2006) Threats to water supplies in the Tropical Andes. *Science* 312:1755–1756
- Buytaert W, Céleri R, De Bièvre B, Cisneros F, Wyseure G, Deckers J, Hofstede R (2006) Human impact on the hydrology of the Andean páramos. *Earth-Sci Rev* 79:53–72
- Castaño C (2002) Páramos y ecosistemas alto andinos de Colombia en condición Hotspot y Global Climatic Tensor. Instituto de Hidrología, Meteorología y Estudios Ambientales (IDEAM), Bogotá
- Departamento de Geografía-Universidad Nacional de Colombia (2005) Escenarios de cambio climático para el territorio colombiano. Fase PDF-B, Integrated National Adaptation Pilot (INAP) - Informe Ejecutivo. Bogotá, Colombia, 19 pp
- Diaz HF, Grosjean M, Graumlich L (2003) Climate variability and change in high elevation regions: past, present and future. In: Diaz HF (ed) Climate variability and change in high elevation regions: past, present and future—Advances in Global Change Research, Kluwer Academic Publishers, 282pp
- Foster P (2001) The potential negative impacts of global climate change on tropical montane cloud forests. *Earth-Sci Rev* 55:73–106
- Gutiérrez H (2002) Aproximación a un modelo para la evaluación de la vulnerabilidad de las coberturas vegetales de Colombia ante un posible cambio climático utilizando Sistemas de Información Geográfica con énfasis en la vulnerabilidad de las coberturas nival y de páramo de Colombia. In: Castaño C (ed.) Páramos y ecosistemas alto andinos de Colombia en condición Hotspot y Global Climatic Tensor. Instituto de Hidrología, Meteorología y Estudios Ambientales (IDEAM), Bogotá, pp 335–377
- Gutiérrez ME, Zapata PA, Ruiz D (2006) Understanding the signals of climate change and climate variability on the water supply of high mountain watersheds (in Spanish). Environmental Engineering Program, School of Engineering, Antioquia, Colombia, 160 pp
- Hastenrath S (1991) Climate dynamics of the tropics. Kluwer, Dordrecht
- Kendall MG (1975) Rank correlation methods. Charles Griffin, London
- Meehl GA, Stocker TF, Collins WD, Friedlingstein P, Gaye AT, Gregory JM, Kitoh A, Knutti R, Murphy JM, Noda A, Raper SCB, Watterson IG, Weaver AJ, Zhao Z-C (2007) Global Climate Projections. In: Climate Change 2007: The Physical Science Basis. Contribution of Working Group I to the Fourth Assessment Report of the Intergovernmental Panel on Climate Change [Solomon S, Qin D, Manning M, Chen Z, Marquis M, Averyt KB, Tignor M, Miller HL (eds)]. Cambridge University Press, Cambridge, United Kingdom and New York, NY, USA, pp 764–765
- Oster R (1979) Precipitation in Colombia (in Spanish). *Revista Colombiana Geográfica*, 6
- Pabón JD (2003) El cambio climático global y su manifestación en Colombia. Cuadernos de Geografía XII (1–2):111–119
- Pabón JD (2004) El cambio climático y sus manifestaciones en Colombia. *Innovación y Ciencia* XI(3–4):68–73
- Rossov WB, Walker AW, Beuschel DE, Roiter MD (1996) International Satellite Cloud Climatology Project (ISCCP) - Documentation of New Cloud Datasets. WMO/TD-No. 737, World Meteorological Organization, p115
- Ruiz D (2009) Signals of climate variability/change in surface water supply of high-mountain watersheds. Case study: Claro River high mountain basin, Los Nevados Natural Park, Andean Central Mountain Range. World Bank Group's Project 7147577. School of Engineering, Medellín, Colombia, p120

- Ruiz D (2010) Indo-Pacific and Tropical Atlantic EOF modes: contributions to the analyses of cloud cover conditions in the Los Nevados Natural Park, Colombian Central Mountain Range. *Revista Escuela de Ingeniería de Antioquia (EIA)*, ISSN 1794–1237, No. 14: 39–52
- Ruiz D, Moreno HA, Gutiérrez ME, Zapata PA (2008) Changing climate and endangered high mountain ecosystems in Colombia. *Science of the Total Environment*. doi:10.1016/j.scitotenv.2008.02.038
- Sen PK (1968) On a class of aligned rank order tests in two-way layouts. *Ann Math Stat* 39:1115–1124
- The World Bank Group (2006) Colombia-Integrated National Adaptation Program Project - Documents & Reports (<http://www.worldbank.org/>).
- The World Bank Group (2008) Assessing the potential consequences of climate destabilization in Latin America. Latin America and Caribbean Region Sustainable Development Working Paper 32 [W. Vergara (ed.)], 115 pp
- Trenberth KE, Jones PD, Ambenje P, Bojariu R, Easterling D, Klein Tank A, Parker D, Rahimzadeh F, Renwick JA, Rusticucci M, Soden B, Zhai P (2007) Observations: Surface and Atmospheric Climate Change. In: *Climate Change 2007: The Physical Science Basis. Contribution of Working Group I to the Fourth Assessment Report of the Intergovernmental Panel on Climate Change* [Solomon S, Qin D, Manning M, Chen Z, Marquis M, Averyt KB, Tignor M, Miller HL (eds)]. Cambridge University Press, Cambridge, United Kingdom and New York, NY, USA, pp 265–271
- Vernekar AD, Kirtman BP, Fennessy MJ (2003) Low-level jets and their effects on the South American summer climate as simulated by the NCEP Eta Model. *J Clim* 16(2):297–311
- Vuille M, Bradley RS, Werner M, Keimig F (2003) 20th century climate change in the Tropical Andes: observations and model results. In: Diaz HF (ed) *Climate variability and change in high elevation regions: past, present and future—Advances in Global Change Research*, Klumer Academic Publishers, 282pp

The views reflected in this article are those of the authors and do not necessarily reflect views of the World Bank Group.